iScience

CellPress
OPEN ACCESS

Article

In situ polymerized ionic liquids in polyester fiber composite membranes for detection of trace oil

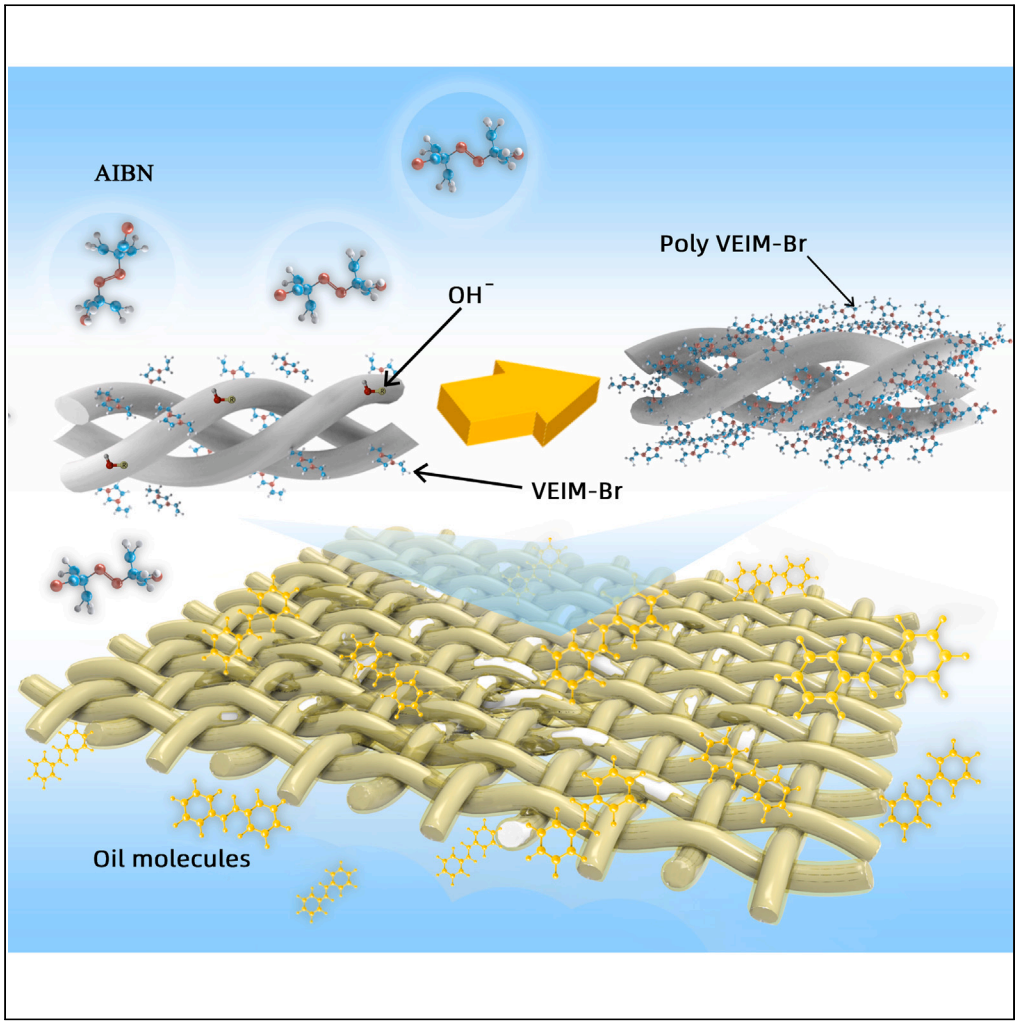

Ruying Wang, Yajing Zheng, Xuejiao Liu, Tongwang Chen, Nan Li, Jing Lin, Jin-Ming Lin

jmlin@mail.tsinghua.edu.cn

Highlights

An ionic liquid-polyester fiber CM for the extraction and detection of trace oil

Combining IL-PF composite membranes (CM) with FT-IR for the analysis of trace oil

The eco-friendly and convenient method has high sensitivity and fast response time

It shows excellent performance in rapid detection of trace oil on metal surface

Wang et al., iScience 26, 106776
June 16, 2023
https://doi.org/10.1016/j.isci.2023.106776

iScience

CellPress
OPEN ACCESS

Article

In situ polymerized ionic liquids in polyester fiber composite membranes for detection of trace oil

Ruying Wang,[1,2] Yajing Zheng,[1,2] Xuejiao Liu,[1] Tongwang Chen,[1] Nan Li,[1] Jing Lin,[1] and Jin-Ming Lin[1,3,*]

SUMMARY

***In situ* trace detection on ultra-clean surfaces is an important technology. The polyester fiber (PF) was introduced to serve as the template, to which the ionic liquids were bonded by hydrogen bonding. Polymerized ionic liquids (PIL) in PF were formed by *in situ* polymerization with the azodiisobutyronitrile (AIBN) and IL. The trace oil on metal surfaces was enriched by the composite membrane based on similar compatibility principle. The absolute recovery of the trace oil ranged from 91%–99% using this composite membrane. In the extraction samples, desirable linear correlations were obtained for trace oil in the range of 1.25–20 mg/mL. It has been proven that a 1 cm^2 PIL-PF composite membrane can effectively extract as little as 1 mg of lubricating oil on an ultra-clean metal surface of 0.1 m^2 with the LOD of 0.9 mg/mL, making it a promising material for *in situ* detection of trace oil on metal surfaces.**

INTRODUCTION

Trace residue lubricant oil can be common in crafts such as electroplating and lacquer tinting, requiring the cleanliness of metal surfaces strictly. It is left on metal surfaces after procedures embracing metal cutting, stretching, forming, etc. The lubricant oil is insoluble in water and retains high viscosity making it tough to wipe thoroughly. Incomplete oil residue cleaning is regarded as the direct cause of poor-quality products since there is no electricity where the oil adheres and the substrate is not firmly bonded consequently.[1] Subsequently, the plate peels off and rust occurs through the action of oxygen and moisture. Hence, detecting and eliminating trace lubricant oil without residue has been extensively explored in industries with abundant ultra-clean surfaces existing.

During these years, many strategies have been proposed for oil/water separation, including physical methodology,[2] chemical methodology,[3] and some materials, for example, ion-imprinted chitosan-base aerogel,[4] melamine sponge,[5] etc. The methods that can be accessed to detect trace oils are generally using fluorescence spectroscopy to detect trace oils in seawater[6] or using visible light LEDs and metal waveguide capillaries to analyze trace oils in water.[7] Not many research studies have been conducted for *in situ* extraction of trace oils on ultra-clean surfaces.

Several of these processes employ environmentally hazardous solvents, such as HCFCs, to extract the oil. Moreover, those approaches employing chemical reactions could induce some impairment to metal plates and had residues left stained on ultra-clean plates. Ionic liquids (ILs) were known as green solvents and widely applied in various fields, e.g., used for functional sequences,[8] enhance solid-state phase microextraction SPME,[9] compliance ion adhesion electrode with ultra-low bio-electron impedance,[10] extraction[11] and separation of oil from oil sands and sludge,[12,13] electrochemistry,[14] graphene materials processing,[15,16] organic synthesis,[17] metal battery,[18–20] desalination,[21,22] etc.[23] ILs own excellent solubility[24] are capable of dissolving diverse organic and inorganic substances. Hence, ILs can be utilized to eliminate lubricant oil, as an alternative to organic solvents. Meanwhile, poly-ionic liquids (PILs) can produce porous films in the form of honeycomb coal,[25] and cellulose happens to be an excellent reaction template.[26] Bacterial cellulose (BC) is a programmable and sustainable environmental material with a three-dimensional mesh structure.[27–29] It is composed of nanofibers crossed internally[30] and can be used as a matrix material[31] to composite with PILs[32,33] to obtain composites with excellent properties. In addition, polyester fiber (PF) is another three-dimensional network material and has numerous hydroxyl groups, which can be well

[1]Department of Chemistry, Beijing Key Laboratory of Microanalytical Methods and Instrumentation, Key Laboratory of Bioorganic Phosphorus Chemistry & Chemical Biology (Ministry of Education), Tsinghua University, Beijing 100084, China

[2]These authors contributed equally

[3]Lead contact

*Correspondence: jmlin@mail.tsinghua.edu.cn

https://doi.org/10.1016/j.isci.2023.106776

modified. Hence, developing an IL-carrier material composite membrane via copolymerization has the potential to detect and eliminate trace oil residues sensitively (Figure 1A).

In this work, the IL 1-vinyl-3-ethyliMidazoliuM broMide (VEIM-Br) was adopted as a reactive monomer, and the BC and PF were selected as two kinds of carrier materials, respectively. The carrier material's surface was flooded with innumerable hydroxyl groups, which served as active sites. VEIM-Br monomer was bonded to the sites by hydrogen bonding, interacting with the N and H atoms of the imidazole ring and absorbed on carrier materials, consequently. Subsequently, the initiator azobisisobutyronitrile (AIBN) was added to the reaction system. The experiments were carried out in a nitrogen atmosphere. The initiator AIBN undergoes homolytic cleavage and forms a pair of primary radicals. The free radical undergoes the addition reaction with a monomer molecule, forming a chain-initiated monomer free radical. After chain growth, VIEM-Br monomers located in and out of carrier materials polymerized into PVIEM-Br. PVIEM-Br and carrier material formed a composite membrane owning a three-dimensional network interpenetrating structure (Figure 1B). It was a new material for eliminating trace lubricant oil according to the similarity compatibility principle. The similarity compatibility principle means that "those with similar structures are easily soluble in each other, and the more similar the structures, the better they dissolve". In addition, extraction and FT-IR characterization were employed to detect trace lubricant oil and evaluate the extraction efficiency. As a result, the kind of ionic liquid-polyester fiber (IL-PF) composed membrane was proved to be capable of eliminating trace lubricant oil and causing no damage to metal plates or the environment.

RESULTS AND DISCUSSION

Synthesis and characterization of IL-BC composite membranes and IL-PF composite membranes

IL-BC composite membranes and IL-PF composite membranes can be obtained by *in situ* polymerization of IL and carrier materials (Figures S1 and S2). These polymerization reactions were all conducted in a nitrogen atmosphere. The initial success of the composite membranes' preparation was assessed using electron microscope imaging. After amounts of experimental comparison (Figure S3), it was summarized as follows: a higher volume of IL led to more uniform mixing, and a lower concentration of IL was required to avoid generating agglomeration. The reason was the concentration of IL monomer was high, so the free radical polymerization reaction was intense. The PIL with a low polymerization degree at the initial reaction was coated on the fiber surface, the bare hydroxyl on the fiber surface decreased, and the cellulose lost the template effect, resulting in agglomeration. With the decrease of the IL monomer concentration, the degree of aggregation decreased, and the morphology of carrier material could be gradually seen. The optimal IL concentration for a 1 cm^2 square composite membrane (Figure S4) was 0.2 mol/L, while the optimum IL volume was 4 mL.

As the result, in general, BC itself was a soft, wrinkly sheet. After being modified with IL, the thin sheet was coated with uniform, thin slurry to harvest IL-BC composite membranes (Figure 2A). PF seemed to be a three-dimensional network of fibers of uniform thickness intertwining. In contrast, IL-PF composite membranes resembled a leaf specimen with visible veins due to the thin and homogeneous PILs coating (Figure 2B). The PILs were securely adhered between the two fibers, bridging the gap among carrier materials, and creating a robust composite membrane.

To further verify the synthesis of composite membranes, the characteristic peaks of PILs and carrier materials could be detected by FT-IR (Figure 2C). Around 2922 cm^{-1} was the stretching vibration peak of the C-H bond, and the peak at about 1028 cm^{-1} was caused by the C-O and C-C stretching vibrations of the sugar ring. These groups correspond to the molecular structure formula of bacterial cellulose. Around 3409 cm^{-1} was the stretching vibration peak of the -OH bond. 1162 cm^{-1} was the in-plane deformation vibration peak of the imidazole ring C-H bond, and 1570 cm^{-1} was the in-plane stretching vibration peak of the imidazole ring C=C and C=N bonds. The existence of these two peaks proved that the polymer has bipolar characteristics. 750 cm^{-1} is the out-of-plane bending vibration peak of the C-H bond of the imidazole ring. The peak at 1451 cm^{-1} was also the characteristic peak of the imidazole ring. It can be seen from Figure 2C that the absorption peaks of composite membranes at 1630 cm^{-1} and 960 cm^{-1} almost disappeared, indicating that the polymerization reaction was successful and that combining the two materials in the composite membranes did not alter the structures of either component. Therefore, based on Fourier transform infrared spectrometer characterization, we draw the following conclusions: First, the IL was combined

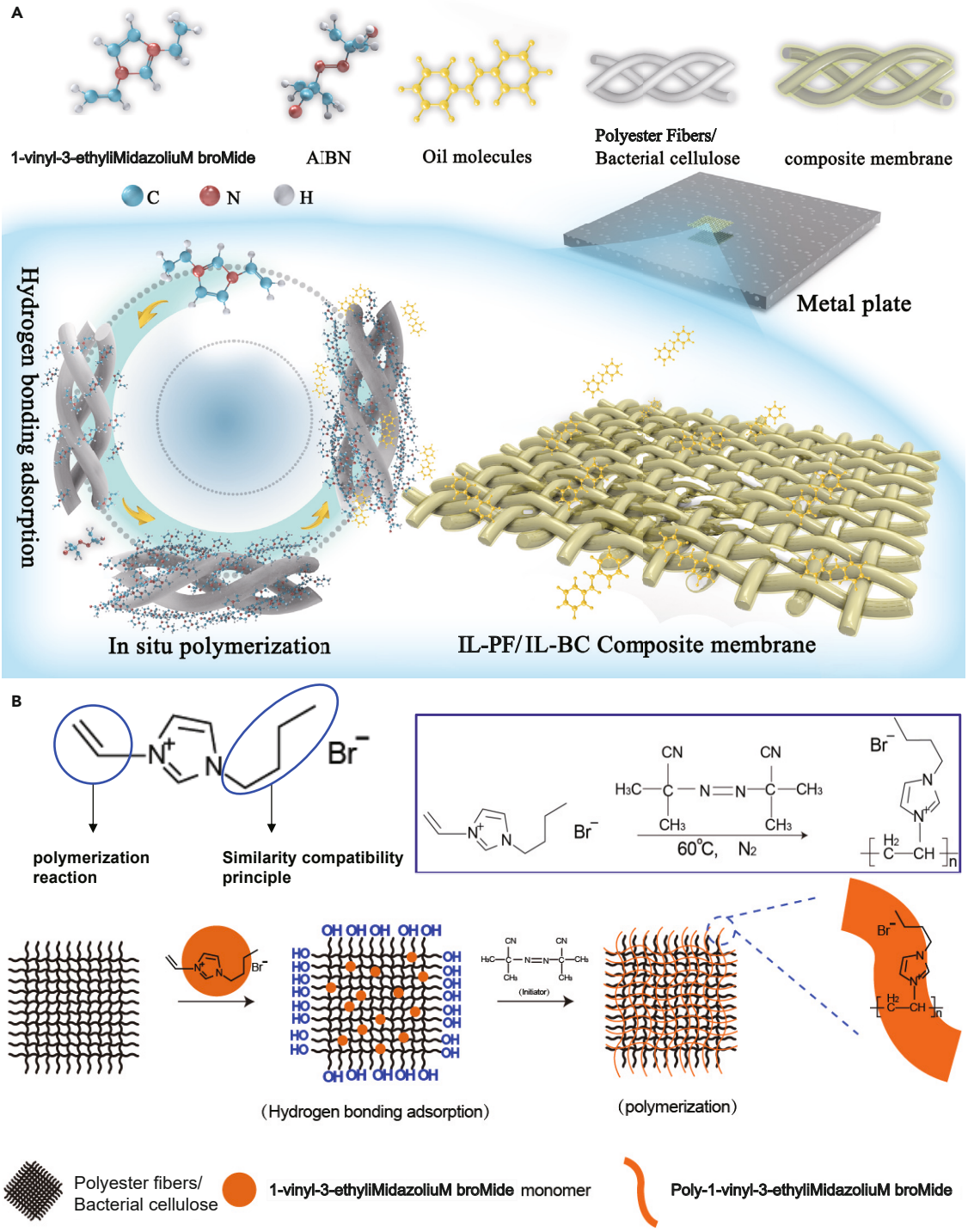

Figure 1. Reaction mechanism of *in situ* polymerization and schematic diagram of oil extraction based on similarity compatibility principle

See also Figure S1 and Figure S2.

(A) Illustration for ionic liquids polymerizing with bacterial cellulose or polyester fiber to form a composite membrane, and extraction of oil molecules by composite membranes.

(B) Chemical reaction mechanism of *in situ* polymerizations of ionic liquids and carrier materials.

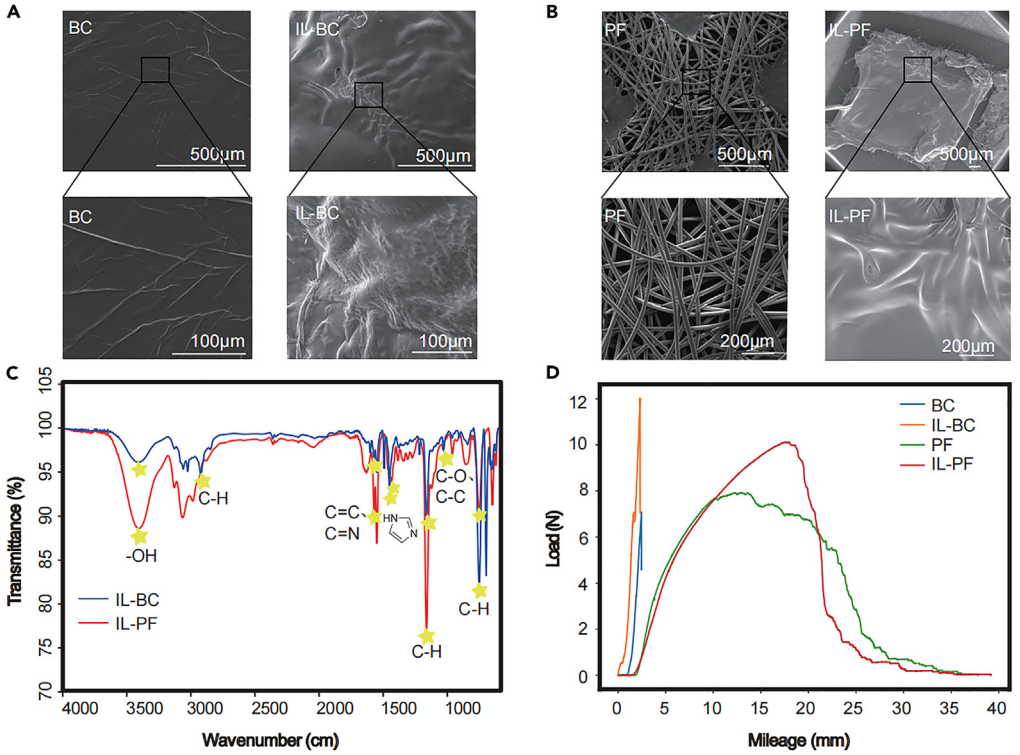

Figure 2. Characterization of composite membranes properties

See also Figure S3 and Figure S4.

(A) Bright-field images comparison of unmodified BC membrane and polymerized IL-BC CMs.

(B) Bright-field images comparison of unmodified PF membrane and polymerized IL-PF CMs.

(C) Infrared spectroscopic characterization of successful polymerization of IL-BC composite membranes and IL-PF composite membranes.

(D) Stress and strain curves of BC membrane, PF membrane, IL-BC composite membrane, and IL-PF composite membrane.

with the carrier material. Moreover, the IL underwent a polymerization reaction to become PILs. Meanwhile, the characteristic peaks of the IL were unaltered, preserving its original function.

Routine detection procedures include checking the film's mechanical characteristics using universal material testing equipment, as seen in Figure 2D. The four samples were BC membrane, PF membrane, IL-BC composite membrane, and IL-PF composite membrane. The size of the samples was 30 mm × 10 mm, and the stretching rate was 5 mm/min. Using BC and PF as carrier materials resulted in IL-BC and IL-PF composite membranes with improved fracture strength and elongation. This is due to the PIL entering the network structure of the carrier material and coating the nanofibers, enhancing the mechanical properties of the original film. At the same time, the PIL could play a plasticizing role in the polymer, which was reflected in the increased elongation at the break of the composite film.

Evaluation of oil extraction effect of the composite membranes

IL-BC composite membranes and IL-PF composite membranes were used to wipe the trace oil. As certified in Figure 3A, there was yellow fluorescence on the surface and inside of the IL-BC composite membrane. Yellow fluorescence also existed in the IL-PF composite membrane as exhibited in Figure 3B, indicating that the PIL was on the surface and inside of the composite membranes, and the oil was successfully extracted.

Furthermore, the two carbon tetrachloride samples (IL-BC composite membranes and IL-PF composite membranes mentioned above) were tested by matrix-assisted laser desorption/ionization-time of flight mass spectrometry (MALDI-TOF).[34] As a comparison, the experiment of using completely unmodified gauze to extract trace oil was done. This gauze was also immersed in carbon tetrachloride as a sample to be tested. Four additional reference samples were prepared, clean IL-BC composite membranes, clean

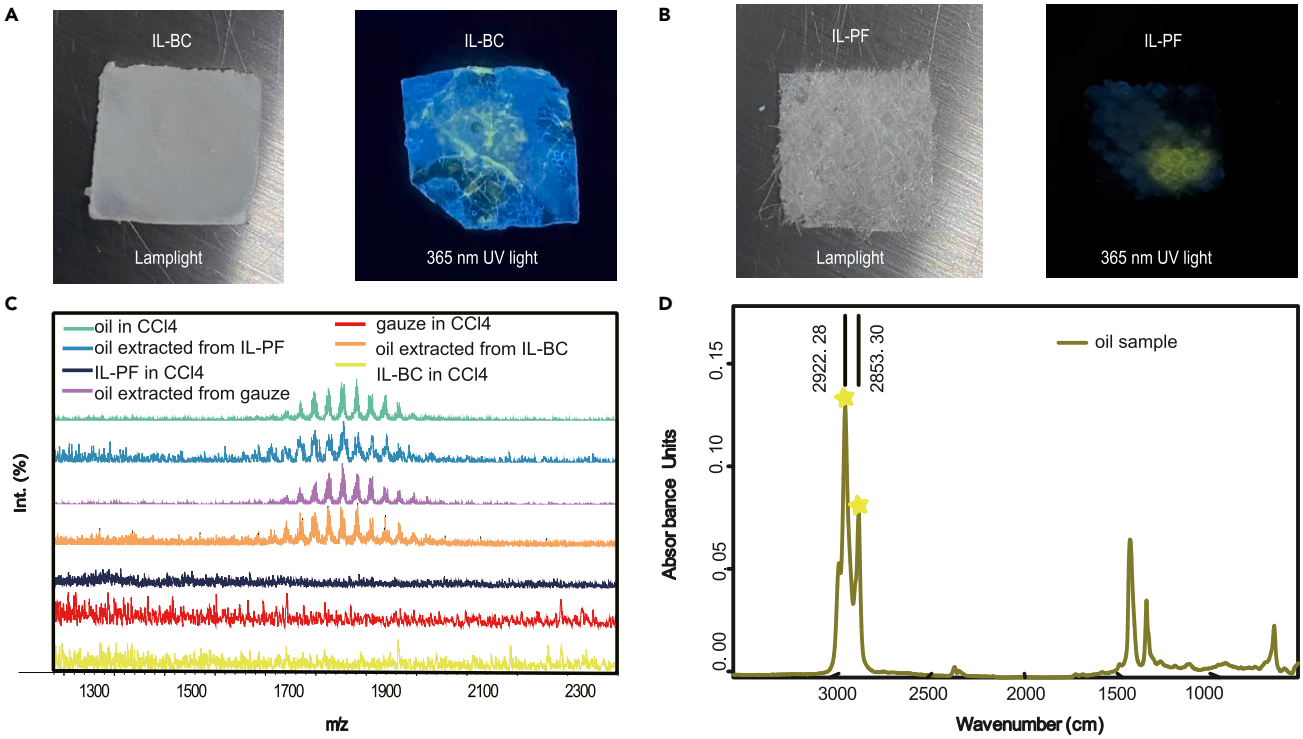

Figure 3. Characterization of the effectiveness of composite membrane extraction of oil by Fluorescence, MALDI-TOF-MASS, and FT-IR

Comparison of photographs of (A) IL-BC composite membrane subjected to oil extraction experiments (right) and original IL-BC composite membrane (left).

(B) IL-PF composite membrane subjected to oil extraction experiments (right) and original IL-PF composite membrane (left).

(C) The MALDI-TOF-MS mass spectrum showed that the standard sample, the composite membranes extraction samples, and the gauze extraction sample all have characteristic peaks.

(D) The infrared spectrum of the oil sample.

IL-PF composite membranes, gauze, and lubricating oil soaked in 800 μL of carbon tetrachloride, respectively. The mass spectra showed identical peaks between *m/z* 1700 to 1900 for the three extraction samples and the lubricant reference sample (Figure 3C). Compared with the extraction samples, the reference samples showed no peak in this range. The molecular weight of carbon tetrachloride is 153.84, which also ruled out this being a peak for carbon tetrachloride. Therefore, it can thus be proved that the composite membranes successfully extracted the trace lubricant from the metal plate.

In addition, the Fourier transform infrared spectrum of the lubricant oil (Figure 3D) showed two distinct absorption peaks at 2853 cm^{-1} and 2922 cm^{-1}, which were selected as the basis for determining the presence of lubricant components.

Quantification of oil extraction of the composite membranes

Absorption peaks of the same mass of trace oil extracted by IL-BC composite membranes and IL-PF composite membranes showed apparent differences (Figures 4A and 4B), indicating that IL-PF composite membranes had a high oil extraction efficiency compared to IL-BC composite membranes.

After this, the oil extraction efficiency of the two composite membranes was further quantified by FT-IR detection. According to Lambert Beer's law, the absorbance (peak area) is proportional to the concentration. The recovery rate was calculated as Oil recovery rate = peak area $_{(Extraction\ Sample)}$/peak area $_{(Standard)}$. According to the above-mentioned formula, the recovery rates of oil in IL-PF composite membranes were calculated by the absorbance peak areas and are shown in Figure 4C. The suggested approach proved accurate and trustworthy for evaluating the trace oil on ultra-clean surfaces, with a complete recovery of 91%–99%. However, IL-BC composite membranes have an oil recovery rate between 55% and 64% (Figure 4D). Two statistical bar charts show that the IL-PF composite membranes were more effective in extracting trace oil than the IL-BC composite membranes, confirming their ability.

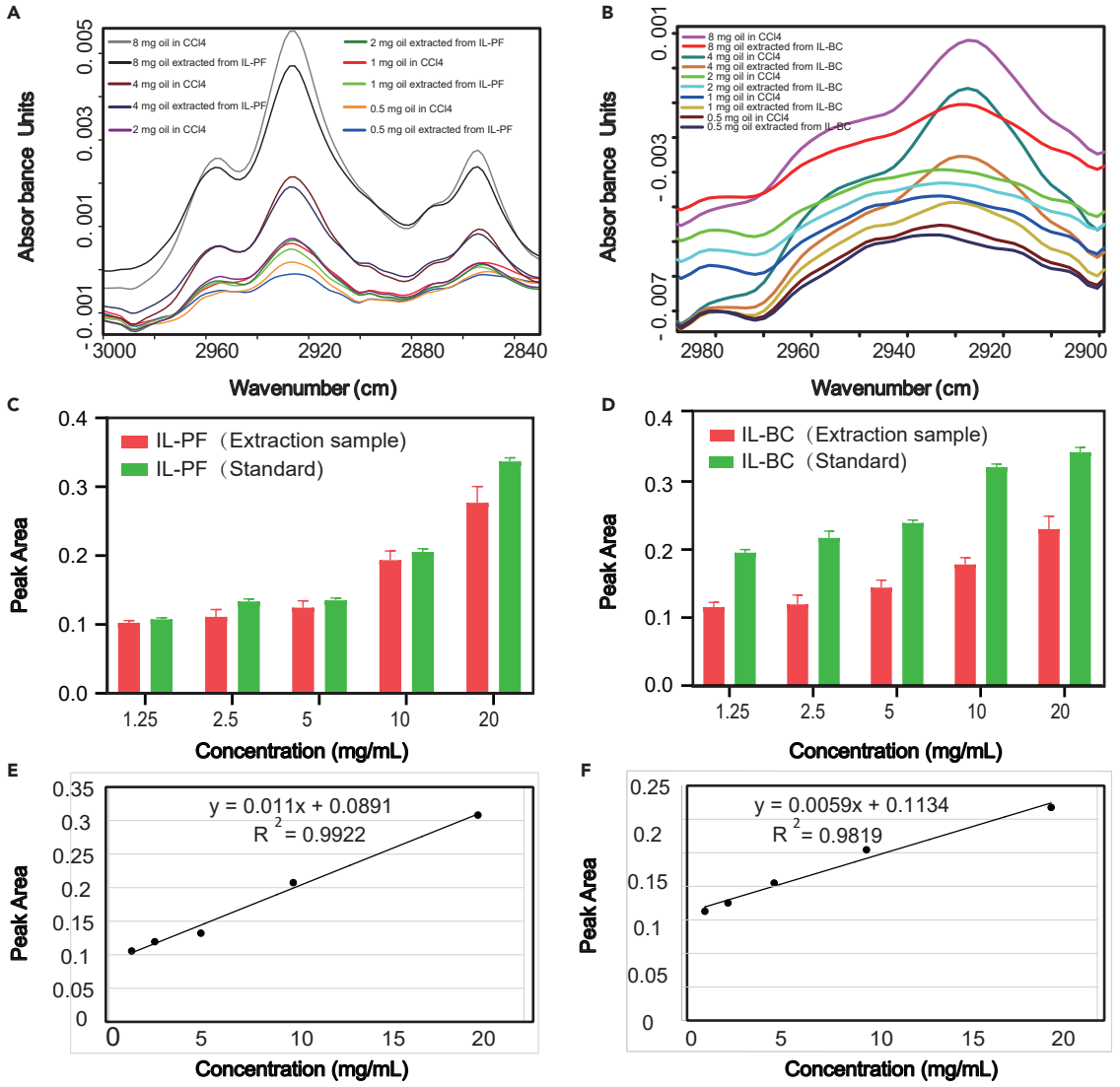

Figure 4. The infrared spectrum of standard samples (0.5 mg, 1 mg, 2 mg, 4 mg, and 8 mg oil were directly mixed with 400 μL of carbon tetrachloride) and extraction samples (0.5 mg, 1 mg, 2 mg, 4 mg, and 8 mg of oil were extracted by

(A) IL-PF composite membranes and (B) IL-BC composite membranes.

(C) FT-IR absorption peak area of standard samples of each concentration and samples extracted by IL-PF composite membranes.

(D) FT-IR absorption peak area of standard samples of each concentration and samples extracted by IL-BC composite membranes.

(E) Standard curve of oil extracted by IL-PF composite membranes.

(F) Standard curve of oil extracted by IL-BC composite membranes.

Data were represented as means ± SEM.

The quantitation of the trace oil was carried out using external standard calibration.[35] The working solution was prepared by extracting oil (0.5 mg, 1 mg, 2 mg, 4 mg, and 8 mg lubricating oil) by IL-PF composite membranes and then immersing membranes into 400 μL carbon tetrachloride (99.5%), yielding concentrations ranging from 1.25 mg/mL to 20 mg/mL. The standard curve of the oil solution was constructed by the mean value of five different concentrations. Each solution has been detected 3 times by scanning continually. The standard curve was obtained as follows: the peak area (Y) of the oil solution increased linearly with the corresponding concentration (X), and the fitting formula is written as follows: Y = (0.011) X + (0.0891). The regression coefficient (R^2) in the calibration curve was higher than 0.99, as shown in Figure 4E, LOD is 0.9 mg/mL calculated based on three times signal-to-noise ratio (S/N = 3). Upon result showed that a desirable linear correlation was obtained for trace oil in the range of 1.25 mg/mL to 20 mg/mL. The standard curve is shown in Figure 4F: Y = (0.0059) X + (0.1134).

Table 1. Comparison of some performance parameters of IL-PF and IL-BC, related to Figure 4

Material	IL-PF	IL-BC
Recovery rate	91%–99%	55%–64%
Liner range	1.25–20 mg/mL	1.25–20 mg/mL
Extraction time	10 min	20 min
Usage count	1 time/piece	1 time/piece
Cost	$0.30/piece	$0.37/piece
The morphology of poly-ionic liquids on carrier materials	Thin and homogeneous	Few and easy to fall off

The regression coefficient (R^2) in the calibration curve was 0.9819. IL-PF composite membranes were chosen for further extraction of trace oil because they were more sensitive than IL-BC composite membranes concerning regression coefficient value and extraction rate (Table 1).

A smear test for the practical use of the IL-PF composite membranes' ability to extract trace oils

A realistic smear test was conducted to evaluate the capability of IL-PF composite membranes to remove trace oil. 1 mg, 2 mg, and 4 mg of lubricating oil were dissolved (respectively) in 3 mL of carbon tetrachloride and then uniformly dusted over (respectively) a 0.1 m^2 of ultra-clean metal plate to mimic the conditions of actual use. After carbon tetrachloride volatilization, oil stains on the ultra-clean metal plate were removed using IL-PF composite membranes. Finally, 800 μL of carbon tetrachloride was used to remove the oil from the composite film, and the resulting IR spectrum was analyzed using FT-IR spectroscopy.

Figure 5A displays the absorption peak spectra of three reference samples and three extraction samples, whereby the area of the absorption peak increases as the concentration of the oil solution rises. The FT-IR absorption peak area was less when the trace oil was diluted and evenly coated on a plate of 0.1 m^2 compared to when the oil was extracted in its whole. The peak area was determined by selecting the absorption peaks from 2900 cm^{-1} to 2980 cm^{-1}. Each sample was tested three times to obtain a histogram as shown in Figure 5B. According to Lambert Beer's law, it can be calculated that the oil extraction rate between 1.25 and 5 mg/mL was between 65% and 70%.

Membranes made from IL-PF composites have a stable composite structure and high oil affinity and are suitable for mass manufacturing. The price of PF was low, and the quantity of initiator and IL monomer needed to prepare the composite membrane was small. This composite membrane can be mass-produced because of its inexpensive cost. IL-PF composite membranes increased the method's feasibility, economy, and operability by using a minimal quantity of adsorbent and a rapid extraction period.

Conclusion

In conclusion, we examined two composite membranes with various carrier materials. We created a composite membrane made of IL and polyester fibers to extract and detect trace oils. The extraction rate was increased, and the potential harm from organic solvent was addressed using IL-PF composite membrane rather than more traditional material.

As a bonus, the use of IL-PF composite membranes simplified real-time extraction and *in situ* detection. Using the *in situ* polymerization approach of the IL-carrier material, we developed a stable and susceptible composite material for trace oil extraction, paving the way for accurate and reliable detection of trace oils.

This material may be fused with a small infrared detector or oil-sensitive fluorescent material to develop a field device for detecting trace oil. This method helps detect and trace oil pollution on the products' surface and serves as a technical reference for verifying the quality of industrial instruments.

Limitations of the study

In this work, only two carrier materials and one IL were experimented. More carrier materials and more ILs can be experimented in further research to improve the extraction sensitivity and optimize the material stability.

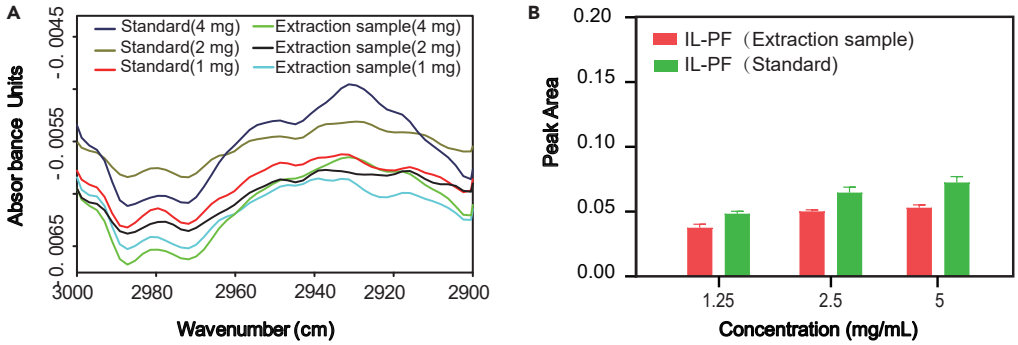

Figure 5. The infrared spectrum and absorption peak area of standard samples and extraction samples of IL-PF composite membranes

(A) In the actual application scenario, the FT-IR spectrum and (B) absorption peak area of standard samples of each concentration and extraction samples of IL-PF composite membranes. Data were represented as means ± SEM.

STAR★METHODS

Detailed methods are provided in the online version of this paper and include the following:

- KEY RESOURCES TABLE
- RESOURCE AVAILABILITY
  - Lead contact
  - Materials availability
  - Data and code availability
- EXPERIMENTAL MODEL AND SUBJECT DETAILS
- METHOD DETAILS
  - Chemicals and materials
  - Characterization
  - Preparation of composite membranes
  - FT-IR characterization
  - Fluorescence characterization
  - MALDI-TOF-MS characterization
  - Semi-quantitative of oil extracted experiment
- QUANTIFICATION AND STATISTICAL ANALYSIS
- ADDITIONAL RESOURCES

SUPPLEMENTAL INFORMATION

Supplemental information can be found online at https://doi.org/10.1016/j.isci.2023.106776.

ACKNOWLEDGMENTS

This work was financially supported by the National Key R&D Program of China (No.2021YFF0600700) and the National Natural Science Foundation of China (Nos. 81973569, 21621003).

AUTHOR CONTRIBUTIONS

All the authors contributed to the work presented in this article. J.L.: Acquisition of the financial support for the project, formulation of overarching research goals and supervised study. Y.Z.: Design of methodology and modified the article. R.W.: Specifically performed the experiments, statistical analysis and drafted the article. R.W. and Y.Z. made equal contributions to this work. X.L. and T.C. also participated in the experiments. J.L. participated in the MALDI-TOF-MS analysis. N.L.: Modified the article.

DECLARATION OF INTERESTS

The authors declare no competing interests.

INCLUSION AND DIVERSITY

We support inclusive, diverse, and equitable conduct of research.

Received: December 5, 2022
Revised: April 6, 2023
Accepted: April 25, 2023
Published: April 29, 2023

REFERENCES

1. Qin, F., Chen, S., Chen, R., Zhan, H., Miao, X., Xiang, W., and Zhao, K. (2021). Leakage detection of oil tank using terahertz spectroscopy. Sci. China Technol. Sci. *64*, 1947–1952. https://doi.org/10.1007/s11431-021-1884-1.

2. Li, M., Bian, C., Yang, G., and Qiang, X. (2019). Facile fabrication of water-based and non-fluorinated superhydrophobic sponge for efficient separation of immiscible oil/water mixture and water-in-oil emulsion. Chem. Eng. J. *368*, 350–358. https://doi.org/10.1016/j.cej.2019.02.176.

3. Aurell, J., and Gullett, B.K. (2010). Aerostat sampling of PCDD/PCDF emissions from the gulf oil spill in situ burns. Environ. Sci. Technol. *44*, 9431–9437. https://doi.org/10.1021/es103554y.

4. Wu, L., Yang, M., Yao, L., He, Z., Yu, J.X., Yin, W., and Chi, R.A. (2022). Polyaminophosphoric acid-modified ion-imprinted chitosan. ACS Appl. Mater. Interfaces *14*, 53947–53959. https://doi.org/10.1021/acsami.2c18163.

5. Wang, H., Zhao, Q., Zhang, K., Wang, F., Zhi, J., and Shan, C.X. (2022). Superhydrophobic nanodiamond-functionalized melamine sponge for oil/water separation. Langmuir *38*, 11304–11313. https://doi.org/10.1021/acs.langmuir.2c01480.

6. Baszanowska, E., and Otremba, Z. (2022). Fluorometric detection of oil traces in a sea water column. Sensors *22*, 2039. https://doi.org/10.3390/s22052039.

7. Bai, M., Huang, H., Yu, Y., Hao, J., Zhang, J., Fan, J., and Yan, J. (2016). Trace analysis of oil-in-water by using visible LED and metal waveguide capillary. Opt Express *24*, 14538–14545. https://doi.org/10.1364/OE.24.014538.

8. Dong, Z., Zhang, C., Peng, H., Gong, J., Wang, H., Zhao, Q., and Yuan, J. (2020). A cationitrile sequence encodes mild poly(ionic liquid) crosslinking for advanced composite membranes. Mater. Horiz. *7*, 2683–2689. https://doi.org/10.1039/D0MH00795A.

9. Patinha, D.J.S., Wang, H., Yuan, J., Rocha, S.M., Silvestre, A.J.D., and Marrucho, I.M. (2020). Thin porous poly(ionic liquid) coatings for enhanced headspace solid phase microextraction. Polymers *12*, 1909. https://doi.org/10.3390/polym12091909.

10. Pan, L., Cai, P., Mei, L., Cheng, Y., Zeng, Y., Wang, M., Wang, T., Jiang, Y., Ji, B., Li, D., and Chen, X. (2020). A compliant ionic adhesive electrode with ultralow bioelectronic impedance. Adv. Mater. *32*, e2003723. https://doi.org/10.1002/adma.202003723.

11. Liu, J., Huang, P., Feng, Q., Lian, P., Liang, Y., Huang, W., Yan, H., and Jia, H. (2019). Systematic investigation of the effects of an anionic surface active ionic liquid on the interfacial tension of a water/crude oil system and its application to enhance crude oil recovery. J. Dispersion Sci. Technol. *40*, 1657–1663. https://doi.org/10.1080/01932691.2018.1527230.

12. Li, X., Sun, W., Wu, G., He, L., Li, H., and Sui, H. (2011). Ionic liquid enhanced solvent extraction for bitumen recovery from oil sands. Energy Fuels *25*, 5224–5231. https://doi.org/10.1021/ef2010942.

13. Williams, P., Lupinsky, A., and Painter, P. (2010). Recovery of bitumen from low-grade oil sands using ionic liquids. Energy Fuels *24*, 2172–2173. https://doi.org/10.1021/ef901384s.

14. Fajardo, O.Y., Bresme, F., Kornyshev, A.A., and Urbakh, M. (2015). Electrotunable lubricity with ionic liquid nanoscale films. Sci. Rep. *5*, 7698. https://doi.org/10.1038/srep07698.

15. Mo, Y., Wan, Y., Chau, A., and Huang, F. (2014). Graphene/ionic liquid composite films and ion exchange. Sci. Rep. *4*, 5466. https://doi.org/10.1038/srep05466.

16. Zhou, X., Zhang, Y., Huang, Z., Lu, D., Zhu, A., and Shi, G. (2016). Ionic liquids modified graphene oxide composites: a high efficient adsorbent for phthalates from aqueous solution. Sci. Rep. *6*, 38417. https://doi.org/10.1038/srep38417.

17. Cao, C.X., Yuan, J., Cheng, J.P., and Han, B.H. (2017). Synthesis of porous polymer/tissue paper hybrid membranes for switchable oil/water separation. Sci. Rep. *7*, 3101. https://doi.org/10.1038/s41598-017-03265-z.

18. Sun, H., Zhu, G., Xu, X., Liao, M., Li, Y.Y., Angell, M., Gu, M., Zhu, Y., Hung, W.H., Li, J., et al. (2019). A safe and non-flflammable sodium metal battery based on an ionic liquid electrolyte. Nat. Commun. *10*, 3302. https://doi.org/10.1038/s41467-019-11102-2.

19. Zhang, J., Sun, B., Zhao, Y., Tkacheva, A., Liu, Z., Yan, K., Guo, X., McDonagh, A.M., Shanmukaraj, D., Wang, C., et al. (2019). A versatile functionalized ionic liquid to boost the solution-mediated performances of lithium-oxygen batteries. Nat. Commun. *10*, 602. https://doi.org/10.1038/s41467-019-08422-8.

20. Rakov, D.A., Chen, F., Ferdousi, S.A., Li, H., Pathirana, T., Simonov, A.N., Howlett, P.C., Atkin, R., and Forsyth, M. (2020). Engineering high-energy-density sodium battery anodes for improved cycling with superconcentrated ionic-liquid electrolytes. Nat. Mater. *19*, 1096–1101. https://doi.org/10.1038/s41563-020-0673-0.

21. Guo, J., Tucker, Z.D., Wang, Y., Ashfeld, B.L., and Luo, T. (2021). Ionic liquid enables highly effificient low temperature desalination by directional solvent extraction. Nat. Commun. *12*, 437. https://doi.org/10.1038/s41467-020-20706-y.

22. Deyab, M.A., and Mohsen, Q. (2021). Corrosion mitigation in desalination plants by ammonium-based ionic liquid. Sci. Rep. *11*, 21435. https://doi.org/10.1038/s41598-021-00925-z.

23. Gunawan, C.A., Ge, M., and Zhao, C. (2014). Robust and versatile ionic liquid microarrays achieved by microcontact printing. Nat. Commun. *5*, 3744. https://doi.org/10.1038/ncomms4744.

24. Liu, J.f., Jiang, G.b., Chi, Y.g., Cai, Y.q., Zhou, Q.x., and Hu, J.T. (2003). Use of ionic liquids for liquid-phase microextraction of polycyclic aromatic hydrocarbons. Anal. Chem. *75*, 5870–5876. https://doi.org/10.1021/ac034506m.

25. Wu, B., Zhang, W., Gao, N., Zhou, M., Liang, Y., Wang, Y., Li, F., and Li, G. (2017). Poly (ionic liquid)-based breath figure films: a new kind of honeycomb porous films with great extendable capability. Sci. Rep. *7*, 13973. https://doi.org/10.1038/s41598-017-14563-x.

26. Zheng, W.l., Hu, W.l., Chen, S.y., Zheng, Y., Zhou, B.h., and Wang, H.p. (2014). High photocatalytic properties of zinc oxide nanoparticles with amidoximated bacterial cellulose nanofibers as templates. Chin. J. Polym. Sci. *32*, 169–176. https://doi.org/10.1007/s10118-014-1386-0.

27. Rakowska, J., Węgrzyn, M., and Rudnik, E. (2021). Impact of ionic liquids on absorption behaviour of natural fbers/biopolyethylene biocomposites. Sci. Rep. *11*, 20483. https://doi.org/10.1038/s41598-021-99956-9.

28. Gilbert, C., Tang, T.C., Ott, W., Dorr, B.A., Shaw, W.M., Sun, G.L., Lu, T.K., and Ellis, T. (2021). Living materials with programmable functionalities grown from engineered microbial co-cultures. Nat. Mater. *20*, 691–700. https://doi.org/10.1038/s41563-020-00857-5.

29. Gao, M., Li, J., Bao, Z., Hu, M., Nian, R., Feng, D., An, D., Li, X., Xian, M., and Zhang, H. (2019). A natural in situ fabrication method of functional bacterial cellulose using a microorganism. Nat. Commun. *10*, 437. https://doi.org/10.1038/s41467-018-07879-3.

30. Thongsomboon, W., Serra, D.O., Possling, A., Hadjineophytou, C., Hengge, R., and Cegelski, L. (2018). Phosphoethanolamine cellulose: a naturally produced chemically modified cellulose. Science *359*, 334–338. https://doi.org/10.1126/science.aao4096.

31. Li, T., Chen, C., Brozena, A.H., Zhu, J.Y., Xu, L., Driemeier, c., Dai, J., Rojas, O.J., Isogai, A., Wågberg, L., and Hu, L. (2021). Developing fibrillated cellulose as a sustainable technological material. Nature *590*, 47–56. https://doi.org/10.1038/s41586-020-03167-7.

32. Ito, A., Yasuda, T., Ma, X., and Watanabe, M. (2017). Sulfonated polyimide/ionic liquid composite membranes for carbon dioxide separation. Polym. J. *49*, 671–676. https://doi.org/10.1038/pj.2017.31.

33. Ahmed, K., Kawakami, M., Khosla, A., and Furukawa, H. (2019). Soft, conductive nanocomposites based on ionic liquids/carbon nanotubes for 3D printing of flflexible electronic devices. Polym. J. *51*, 511–521. https://doi.org/10.1038/s41428-018-0166-z.

34. Bell, S.E., Park, I., Rubakhin, S.S., Bashir, R., Vlasov, Y., and Sweedler, J.V. (2021). Droplet microfluidics with MALDI-MS detection: the effffects of oil phases in GABA analysis. ACS Meas. Sci. Au *1*, 147–156. https://doi.org/10.1021/acsmeasuresciau.1c00017.

35. Xu, G., Hou, L., Liu, C., Wang, X., Liu, L., Li, N., Lin, J.M., and Zhao, R.S. (2021). Fabrication of a magnetic fluorinated covalent organic framework for the selective capture of benzoylurea insecticide residue in beverages. ACS Appl. Mater. Interfaces *13*, 51535–51545. https://doi.org/10.1021/acsami.1c15869.

36. Han, J., Li, Q., Tan, L., Chen, S., and Wang, H. (2015). Preparation and properties of electromagnetic funtional composite membrane based on bacterial cellulose. Gongneng Cailiao *46*, 14083–14087. https://doi.org/10.3969/j.issn.1001-9731.2015.14.016.

STAR★METHODS

KEY RESOURCES TABLE

REAGENT or RESOURCE	SOURCE	IDENTIFIER
Chemicals, peptides, and recombinant proteins		
2-methylpropionitrile	J&K Scientific Ltd	CAS#:78-67-1
1-vinyl-3-ethyliMidazoliuM broMide	MERYER	CAS#:81517-60-4
Trichloromethane	Beijing Tongguang Fine Chemical Company	CAS#:67-66-3
Fluorescent Yellow 131SC Liquid Dye	Dow Chemical (Shanghai, China) Co	N/A
Carbon tetrachloride (99.5%)	Adamas	CAS#:56-23-5
Bacterial cellulose film	Shanghai PZ Bio-Tech Co. Ltd	N/A
Polyester fiber film	Shanghai PZ Bio-Tech Co. Ltd	N/A
Lubricant oil (Mobil 5W-40)	ExxonMobil (China) Investment Co. Ltd	N/A
Ethyl alcohol	Beijing Century Better Technology Development Co. Ltd	CAS#:swaxk71487
Software and algorithms		
Origin	OriginLab	www.originlab.com
Other		
Quanta 200	Netherlands	N/A
20 KN WDW3020	Changchun Kexin Experimental Instrument Company	N/A
FT-IR	Bruker	N/A
MALDI-TOF-MS	Shimadzu	N/A

RESOURCE AVAILABILITY

Lead contact

Further information and requests for resources and reagents should be directed to and will be fulfilled by the lead contact, Jin-Ming Lin (jmlin@mail.tsinghua.edu.cn).

Materials availability

This study did not generate new unique reagents.

Data and code availability

- Data reported in this paper will be shared by the lead contact upon reasonable request.
- This study does not report any original code.
- Any additional information required to reanalyze the data reported in this paper is available from the lead contact upon reasonable request.

EXPERIMENTAL MODEL AND SUBJECT DETAILS

This study does not use experimental models.

METHOD DETAILS

Chemicals and materials

2-methylpropionitrile was provided by J&K Scientific Ltd. (Beijing, China). 1-vinyl-3-ethyliMidazoliuM bro-Mide was purchased from Beijing Huawei Ruike Chemical Co. Ltd. (Beijing, China). Trichloromethane was obtained from Beijing Tongguang Fine Chemical Company (Beijing, China). Carbon tetrachloride (99.5%) was supplied by Shanghai Titan Technology Co. Ltd. (Shanghai, Beijing). Bacterial cellulose film and PF film were acquired from Shanghai PZ Bio-Tech Co. Ltd (Shanghai, China). Fluorescent Yellow 131SC Liquid Dye

was provided by Dow Chemical (Shanghai, China) Co. Lubricant oil (Mobil 5W-40) was bought from ExxonMobil (China) Investment Co. Ltd. (Shanghai, China). Ethyl alcohol was obtained from Beijing Century Better Technology Development Co. Ltd. (Beijing, China).

Characterization

Scanning electron microscope (SEM) characterization

The instrument used to observe and characterize the synthesis of composite membranes was an environmental scanning electron microscope. All electron micrographs in this work were made using a Quanta 200 environmental scanning electron microscope from the Netherlands with resolutions of 10 nm (high vacuum mode, 30 kV), 20 nm (low vacuum mode, 30 kV), 200 nm (ESEM environmental vacuum mode, 30 kV), 50nm (low vacuum mode, 3 kV). Magnification: 7-1000,000 ×. Maximum pixel: 3584 × 3094.

Stress and strain characterization

The 20 KN WDW3020 universal testing machine produced by Changchun Kexin Experimental Instrument Company was used in this experiment. The maximum experimental stress was 20 KN, the speed range of moving beam was 0.005~500 mm/min, the displacement resolution of moving beam was 0.001 mm, and the maximum travel of moving beam was 1100 mm.

Preparation of composite membranes

Since polymerization of double bonds can lengthen molecular chains, and since the increased carbon chain structure is assumed to have a high extracting capacity based on similarity compatibility, an IL with a double bond and a long carbon chain was selected as a further step. Bacterial cellulose and polyester fibers were selected as the carrier material. The next step is to add monomers of IL, which cling to the surface of bacterial cellulose and polyester fibers due to hydrogen bonding. The polymerization process was carried out at 60 °C after applying the initiator. The IL monomer was polymerized into long chains on the carrier material, and finally, a stable three-dimensional network interpenetration structure was obtained (Figure S5). Cropping the bacterial cellulose membranes and polyester fibers membranes to 1 cm × 1 cm, which was the size required for this experiment. To activate the bacterial cellulose membranes and polyester fibers membranes, they were first soaked in ethyl alcohol for 10 min and then transferred into chloroform in a 10 mL reaction flask and stored at room temperature. After several minutes, the bacterial cellulose membranes and polyester fibers membranes swelled, allowing the VEIM-Br monomer to diffuse into the three-dimensional porous network structure of bacterial cellulose and polyester fibers through soaking. Ionic liquids were synthesized according to the reported literature.[36]

1-Ethenyl-3-ethylimidazole bromide salt was selected as the reactive monomer. In a 10 mL reaction flask, 0.4 g of bromide salt of 1-ethenyl-3-ethyl imidazole was dissolved in 10 mL of chloroform with continuous shaking for full dissolution. After placing the IL (4 mL) in the reaction flask (10 mL), 2 pieces of bacterial cellulose membranes or PF membranes were added. The monomer can use hydroxyl as the active site, interact with the N and H atoms in the imidazole ring through hydrogen bonds, and adsorb on the surface of the bacterial cellulose nanofibers or polyester fibers. After that, 12 mg of initiator AIBN was added and shaken uniformly at 60 °C for 2 h. Nitrogen provided assured safety for the reaction system. After gently washing three times with the chloroform and drying in a fume hood, the solid white product was harvested by free radical polymerization.

In the polymerization reaction, different sizes of bacterial cellulose membranes and polyester fibers membranes required different IL concentrations, volumes, and initiator concentrations. Herein, it is necessary to seek out the optimal polymerization conditions for different sizes and different materials of composite membranes. To prepare IL-BC composite membranes and IL-PF composite membranes with different ILs, a series of 0.4 g, 0.6 g, and 0.8 g IL monomers were weighed and then ultrasonically mixed with 10 mL of chloroform, respectively (0.2 mol/L, 0.3 mol/L, and 0.4 mol/L of ILs were configured respectively). To make a 1 cm × 1 cm IL-BC composite membrane or IL-PF composite membrane, first, a 1 cm × 1 cm piece of bacterial cellulose membrane or polyester fibers membrane was cut as a template. After that, 2 mL, 3 mL, and 4 mL of ILs of different concentrations were dispensed, and two 1 cm × 1 cm bacterial cellulose membranes or two IL-PF composite membranes were placed in each reaction bottle which was shaken continuously for more than 12 hours at room temperature. After the IL and the carrier materials were completely combined, the initiator AIBN was added at a concentration of 3 mg/mL. The reaction

was continued in a constant temperature shaker for 2 h at 60 °C. After the reaction was completed, the IL-BC composite membranes and IL-PF composite membranes were taken out, and after waiting for cooling to room temperature, the IL that did not undergo reaction on the surface of the composite membranes was washed out gently with chloroform.

The IL-BC composite membranes and IL-PF composite membranes were harvested by placing the composite membranes in a fume hood to completely evaporate the chloroform. Observation of the samples with a Quanta 200 environmental scanning electron microscope revealed that the composite membranes prepared with different concentrations of ILs performed diversely.

FT-IR characterization

The infrared spectra of the samples were characterized using Fourier Transform Infrared Spectroscopy (FT-IR). In this experiment, the Bruker infrared spectrometer, manufactured by Horiba, Germany, was used for the infrared characterization, with a spectral range of 8,000-350 cm^{-1}; the resolution was better than 0.16 cm^{-1}; and the number of scans was 64, the scan rate was 4 cm^{-1} /s, and the scan mode was MIR-ATR.XPM.; FT-IR was used to analyze the vibrations of individual functional groups of composite membranes to characterize the polymerization of ILs with bacterial cellulose membranes and polyester fibers.

Prior to analysis, the composite membrane is tested to see if PIL is firmly bound to the carrier material. The ultra-clean metal plate was wiped with the composite membranes strenuously and immersed in 400 μL of carbon tetrachloride for 15 min. Typically, the sample was oscillated sufficiently to dissolve the residue on the metal plate in carbon tetrachloride. Finally, the sample was infused into the FT-IR to detect whether IL components remained (Figure S6).

Fluorescence characterization

Based on the used concentration (300 mg/L) of fluorescent tracer (Fluorescent Yellow 131SC Liquid Dye), and the density ρ=0.85, it can be calculated that to configure 10 g of fluorescent oil, 25.8 μL of fluorescent tracer needs to be added to 11 mL of lubricating oil. An amount of 10 g of lubricating oil was mixed with 25.8 μL of fluorescent liquid dye before being shaken well so that the fluorescent tracer was completely dissolved in the lubricant. The configured fluorescent oil is light orange.

Dropped 0.5 mg of fluorescent oil on the metal plate, and gently wiped the fluorescence on the metal surface by pressing a piece of 1 cm × 1 cm composite membrane with a medical small tweezer. The composite membranes were arranged in sequence under a 365 nm UV lamp, and photographs of the composite membranes were recorded.

MALDI-TOF-MS characterization

The mass spectral data of the composite membrane extracted lubricant were obtained on a MALDI-TOF mass spectrometer. The AXIMA-Performance MA mass spectrometer used in this experiment was produced by Shimadzu, Japan. The ionization source was a matrix-assisted laser desorption ionization source with two detection modes, linear and reflection, and the laser wavelength was 337 nm. Linear detection was used for the sample testing, and the mass range was selected as 1400-2400 m/z. MALDI-TOF was mainly used to examine the effect of membranes extraction of lubricating oil in this experiment. A 10 ml vial containing IL and bacterial cellulose membrane and polyester fibers was placed in a thermostatic shaker for the reaction at a temperature of 60 °C and a speed of 120 rpm.

Semi-quantitative of oil extracted experiment

A series of 0.5 mg, 1 mg, 2 mg, 4 mg, and 8 mg lubricating oil spots were extracted by IL-BC composite membranes and IL-PF composite membranes, respectively. These extracted samples were further immersed in 400 μL of carbon tetrachloride to dissolve oil in carbon tetrachloride. For comparison, 0.5 mg, 1 mg, 2 mg, 4 mg, and 8 mg lubricating oil were directly mixed with 400 μL of carbon tetrachloride, as the standard samples.

Finally, 20 μL samples were taken for IR spectroscopy analysis. FT-IR signals between 600 cm^{-1} and 4000 cm^{-1} were collected in the transmittance mode. For analyzing the efficiency of extracting trace lubricant oil, signals between 2800 cm^{-1} to 3200 cm^{-1} were collected in the absorbance mode to calculate the

peak areas of each group. According to Lambert Beer's Law, the absorbance (peak area) is proportional to the concentration. Therefore, we were able to obtain the extraction rate by calculating the ratio of the peak areas (S_e/S_o, where S_e is the extraction sample's peak area and S_o is the oil sample's peak area).

Test the performance of this material in practical applications. Firstly, the prepared oil dilution solution (1 mg, 2 mg, and 4 mg of oil diluted with 3 mL of carbon tetrachloride) was applied evenly on a 0.1 m^2 metal plate with a pipette gun until the whole metal plate was covered by the oil solution. After the carbon tetrachloride has completely evaporated, wiped the oil spot that remained on the metal surface gently (use two pieces of 1 cm × 1 cm IL-PF composite membranes in sequence). When the extraction of trace oil was completed, two composite membranes were immersed in 800 μL of carbon tetrachloride and placed on an oscillator for 5 h with constant oscillation for extraction.

QUANTIFICATION AND STATISTICAL ANALYSIS

This study use Excel and Origin for statistical analysis or quantification. The statistical details of experiments is available from the lead contact upon request.

ADDITIONAL RESOURCES

This study has not generated or contributed to a new website/forum and it is not part of a clinical trial.